We are IntechOpen, the world's leading publisher of Open Access books Built by scientists, for scientists

6,900
Open access books available

186,000
International authors and editors

200M
Downloads

Our authors are among the

154
Countries delivered to

TOP 1%
most cited scientists

12.2%
Contributors from top 500 universities

CLARIVATE ANALYTICS
BOOK CITATION INDEX
INDEXED

WEB OF SCIENCE™

Selection of our books indexed in the Book Citation Index
in Web of Science™ Core Collection (BKCI)

Interested in publishing with us?
Contact book.department@intechopen.com

Numbers displayed above are based on latest data collected.
For more information visit www.intechopen.com

15

Heat Transfer Enhancement for Weakly Oscillating Flows

Efrén M. Benavides
Universidad Politécnica de Madrid
Spain

1. Introduction

Heat exchangers that work with an oscillatory fluid flow exhibit a heat transfer dependence on the oscillation parameters, and hence such devices can modify its range of applicability and its performances by changing the oscillation parameters. This capability of oscillating flows to modulate the heat transfer process of some devices makes them interesting for some applications. Among the current devices that use oscillating flows are thermoacoustic engines and refrigerators (Backhaus & Swift, 2000; Gardner & Swift, 2003; Ueda et al., 2004), oscillatory flow reactors (Lee et al., 2001; Harvey et al., 2003), and, in general, any kind of heat exchangers with a periodical mass flow rate (Benavides, 2009). The theoretical characterization of the heat transfer process in such devices, where an oscillating flow is imposed over a stationary flow, is necessary either because it appears in a natural way such as in some kind of thermoacoustic devices (Benavides, 2006, 2007) or well because it is forced by pulsating the flow with vibrating or moving parts placed far enough in the upstream or downstream path (Wakeland & Keolian, 2004a, 2004b). Since the heat exchanged depends on the heat fluxes, an interesting way to modify these fluxes could be to change the mean velocity of the fluid just as it has been experimentally corroborated in baffled pipes (Mackley & Stonestreet, 1995). Other interesting way of changing the flux of heat is to change the amplitude and the frequency of an imposed pulsation. Yu et al. (2004) summarize this situation by classifying previous works into four categories according to the conclusion being reached: (a) pulsation enhances heat transfer (Mackley & Stonestreet, 1995; Faghri et al., 1979) (b) pulsation deteriorates heat transfer (Hemida et al., 2002) (c) pulsation does not affect heat transfer (Yu et al., 2004), and (d) heat transfer enhancement or deterioration may occur depending on the flow parameters (Cho & Hyun, 1990). Although, the main conclusion reached by Yu et al. (2004) was that pulsation neither enhances nor deteriorates heat flow and that the same result was found by Chattopadhyay et al. (2006), who showed that pulsation has no effect on the time-averaged heat transfer along straight channels, other results show that forced flow pulsation enhances convective mixing and affects Nusselt number (Kim & Kang, 1998; Velazquez et al., 2007). These works show how the heat transfer reaches its maximum for a specific frequency of oscillation and decreases for both higher and lower values of frequency. This disparity of results motivated a theoretical study (Benavides, 2009), based on a second order expansion of the integral equations that governs the oscillating flow, which predicts the possibility of having heat transfer enhancement or deterioration as a function of the frequency of the oscillation. It is

interesting to note that this feature is present even in the case of having flows where the amplitude of the velocity oscillation is small when it is compared with the time-averaged velocity inside the device. Although the model proposed in that article is highly simplified, it fixes the basic mechanisms leading to a heat transfer enhancement when a pulsating flow is present and hence it gives a common explanation to all the aforementioned results. Here, we discuss this model with the purpose of *i*) obtaining a final formula able to fit the frequency response, and *ii*) showing that a correct measurement of the heat transferred requires a dynamic characterization of the outlet mass flow rate and temperature.

2. Problem formulation

2.1 Characterization of the heat transfer coefficient for weakly oscillating flows

For an incompressible flow under the assumption that the properties of the fluid are temperature independent, the dimensionless form of the conservation laws are given by the following partial derivative equations (Baehr & Stephan, 2006):

$$\sum_{i=1}^{3} \partial_i \upsilon_i = 0 \tag{1}$$

$$\mathrm{St}\,\partial_0 \upsilon_j + \sum_{i=1}^{3} \upsilon_i \partial_i \upsilon_j = -\partial_j p + \frac{1}{\mathrm{Re}} \sum_{i=1}^{3} \partial_i \partial_i \upsilon_j \tag{2}$$

$$\mathrm{St}\,\partial_0 \theta + \sum_{i=1}^{3} \upsilon_i \partial_i \theta = \frac{1}{\mathrm{Pe}} \sum_{i=1}^{3} \partial_i \partial_i \theta + \frac{\mathrm{Ec}}{\mathrm{Re}} \sum_{i=1}^{3} \sum_{j=1}^{3} \partial_j \upsilon_i (\partial_i \upsilon_j + \partial_j \upsilon_i) \tag{3}$$

In these equations, non-dimensional variables are related to dimensional ones by means of the followings relations (dimensional variables are on the left-hand side of the equalities):

$$\omega t = \xi_0 \quad ; \quad \frac{x_i}{L} = \xi_i \quad ; \quad \frac{u_i}{U} = \upsilon_i \quad ; \quad \frac{P}{\frac{1}{2}\rho U^2} = p \quad ; \quad \frac{T_W - T}{T_W - T_L} = \theta(T) \tag{4}$$

$$\omega^{-1} \frac{\partial}{\partial t} = \partial_0 \quad ; \quad L \frac{\partial}{\partial x_i} = \partial_i \tag{5}$$

$$\frac{\omega L}{U} = \mathrm{St} \quad ; \quad \frac{\rho L U}{\mu} = \mathrm{Re} \quad ; \quad \frac{\rho L U c}{k} = \mathrm{Pe} \quad ; \quad \frac{U^2}{c(T_W - T_L)} = \mathrm{Ec} \quad ; \quad \frac{c\mu}{k} = \frac{\mathrm{Re}}{\mathrm{Pe}} = \mathrm{Pr} \tag{6}$$

Here, *t* is the time, x_i are the spatial coordinates, u_i are the fluid velocities, and *P* and *T* are, respectively, the pressure and the temperature of the fluid at time *t* and position x_i; ω is the angular frequency of the oscillation, *L* is a characteristic length of the device, *U* is a characteristic velocity, T_W is the temperature of the hottest surface of the device, T_L is the inlet fluid temperature; ρ, μ, *k*, and *c* are, respectively, the density, the viscosity, the thermal conductivity, and the specific heat capacity of the fluid. Note that the dimensionless numbers St, Re, Pe, and Ec in Eqs. (6) are evaluated as characteristic constant numbers, and hence do not change with the oscillation. Eckert number, Ec, does not depend on the size of

the device (i.e., on the characteristic length, *L*). Besides, it only affects Eq. (3), which is the one governing the temperature field, and only has to be taken into account when friction gives rise to a noticeable warming of the fluid, which is not the case because the kinetic energy is considered to be negligible when compared with the increment of the internal energy due to heat transfer. The order of magnitude of the third term, compared with the heat conduction term in Eq. (3), is given by the dimensionless number:

$$\frac{\text{Pe Ec}}{\text{Re}} = \frac{\mu U^2}{k(T_W - T_L)} = \text{Pr} \frac{U^2}{c(T_W - T_L)} \tag{7}$$

This expression allows defining the following characteristic velocity, whose values at different temperatures are given for water and air in Tables 1 and 2 respectively:

$$U_c = \sqrt{\frac{c(T_W - T_L)}{\text{Pr}}} \tag{8}$$

T	ρ	c	μ	k	Pr	U_c T_W-T_L=1°C	U_c T_W-T_L=10°C
°C	kg m⁻³	J kg⁻¹ K⁻¹	Pa s	W K⁻¹ m⁻¹		m s⁻¹	m s⁻¹
10	999.70	4192.1	1307 ·10⁻⁶	0.5800	9.447	21.2	66.6
50	988.03	4180.6	547.0 ·10⁻⁶	0.6435	3.554	34.3	108
90	965.35	4205.0	314.5 ·10⁻⁶	0.6753	1.958	46.3	147

Table 1. Properties of liquid water at three different temperatures (elaborated from Lide, 2004)

T	ρ	c	μ	k	Pr	U_c T_W-T_L=1°C	U_c T_W-T_L=10°C
K	kg m⁻³	J kg⁻¹ K⁻¹	Pa s	W K⁻¹ m⁻¹		m s⁻¹	m s⁻¹
200	1.746	1007	13.3 ·10⁻⁶	0.0184	0.728	37.2	117.6
300	1.161	1007	18.6 ·10⁻⁶	0.0262	0.715	37.5	118.7
500	0.696	1030	27.1 ·10⁻⁶	0.0397	0.703	38.3	121.0

Table 2. Properties of air (1 bar) at three different temperatures (elaborated from Lide, 2004)

Equations (7) and (8) state that the last term in Eq. (3) can be neglected when $U \ll U_c$. If this term is drooped, an error in the calculated temperature appears. Values collected in Table 1 show that the error is of the order of 1°C for water and a characteristic velocity near 20 m/s (a similar error is obtained for air with a characteristic velocity near 38 m/s). If the characteristic velocity is increased, the error grows: for water at a characteristic velocity near 67 m/s, the order of magnitude of the error is 10°C. When the characteristic velocities inside the device are much less than those given by Tables 1 and 2, the error in the temperature due to neglect this term is much less than 1°C (or 10°C). This means an error less than 1% (or 10%) for water suffering a heating in the range 10-90°C. Note that the errors due to consider that the fluid properties are independent of temperature are greater than these (Table 1 shows that the thermal conductivity of water suffers a variation of 15% in the rage 10-90°C). Thus, the energy equation can be substituted by:

$$\mathrm{St}\,\partial_0\theta + \sum_{i=1}^{3}\upsilon_i\partial_i\theta = \frac{1}{\mathrm{Pe}}\sum_{i=1}^{3}\partial_i\partial_i\theta \tag{9}$$

The remaining numbers, St, Re, and Pe, depend on the size of the device, L. The Strouhal number, St, typically is near one in these applications, and hence the complete device cannot be treated as stationary. However, the Reynolds number, Re, is normally much greater than one. Since, as can be seen in Tables 1 and 2, the Prandtl number, Pr, is not much less than one (for air it is near 0.7 and for water lies in the range 2-10), the Péclet number, Pe, is also much greater than one. This means that the viscosity and the thermal conductivity lead to negligible effects in regions with characteristic lengths of the order of L. However, their effects are stronger in regions with a characteristic length much less than L. In order to see this, it is convenient to introduce these numbers as a function of a characteristic length, l_c, as:

$$\mathrm{St}(l_c) = \frac{\omega l_c}{U} \quad ; \quad \mathrm{Re}(l_c) = \frac{\rho l_c U}{\mu} \quad ; \quad \mathrm{Pe}(l_c) = \mathrm{Re}(l_c)\mathrm{Pr} \tag{10}$$

Indeed, these numbers fix the thickness of the thermal and viscous convective boundary layers. We define the characteristic thickness of the viscous boundary layer as $\mathrm{Re}(\delta_\mu)=1$, which leads to $\delta_\mu=\mu/(\rho U)$. In the same way, the characteristic thickness of the thermal convective boundary layer is defined by $\mathrm{Pe}(\delta_k)=1$, which leads to $\delta_k=k/(\rho c U)$. The conditions $\mathrm{Re}(L)\gg1$ and $\mathrm{Pe}(L)\gg1$ lead to $\delta_\mu\ll L$ and $\delta_k\ll L$, respectively. Therefore, the characteristic thicknesses of the boundary layers are much smaller than the characteristic length of the device. Although, the Strouhal number is typically near one in the device scale, i.e., $\mathrm{St}(L)\sim1$, the Strouhal number in the boundary layers is much less than one, i.e., $\mathrm{St}(\delta_\mu)\ll1$ and $\mathrm{St}(\delta_k)\ll1$. Table 3 collects the different orders of magnitude of the dimensionless numbers $\mathrm{St}(l_c)$, $\mathrm{Re}(l_c)$, and $\mathrm{Pe}(l_c)$, for the three different length scales.

l_c	$\mathrm{St}(l_c)$	$\mathrm{Re}(l_c)$	$\mathrm{Pe}(l_c)$
L	1	$\gg1$	$\gg1$
δ_μ	$\ll1$	1	Pr
δ_k	$\ll1$	Pr^{-1}	1

Table 3. Orders of magnitude of the dimensionless numbers St, Re, and Pe, as a function of the length scale.

As a consequence of the results shown in the first column of Table 3, the boundary layers can be modeled as quasi-steady. Additionally, the dominant effects in the heat transfer forced by the wall temperature can be restricted to those that are important in a region near the wall that accomplishes $\mathrm{Pe}(l_c)\sim1$. The energy equation can be rewritten for this layer by substituting the characteristic length L wih $\delta_k\ll L$, so that, near the wall, $\mathrm{St}(\delta_k)\sim0(\delta_k/L)\ll1$. The same happens with the viscous boundary layer. This fact allows the removal of the temporal derivatives from the momentum and energy equations that describe the behaviour of the fluid near the wall. Therefore, although the complete device is not stationary, the thermal boundary layers can be modeled as quasi-steady, and Eqs. (2) and (9) can be reduced to:

$$\sum_{i=1}^{3}\upsilon_i\partial_i\upsilon_j = -\partial_j p + \mathrm{Pr}\sum_{i=1}^{3}\partial_i\partial_i\upsilon_j \tag{11}$$

$$\sum_{i=1}^{3} \upsilon_i \partial_i \theta = \sum_{i=1}^{3} \partial_i \partial_i \theta \qquad (12)$$

Let us introduce a local frame of reference in the wall which has the component i=1 parallel to the velocity, the component i=2 perpendicular to the surface wall, and i=3 parallel to the surface wall and perpendicular to the velocity. In this situation, the thermal conduction in the direction of the flow (i=1) can be neglected as well as all the derivatives in the third component (i=3), and hence, the equations are:

$$\upsilon_1 \partial_1 \upsilon_1 = -\partial_1 p + \Pr \partial_2 \partial_2 \upsilon_1 \qquad (13)$$

$$\upsilon_1 \partial_1 \theta = \partial_2 \partial_2 \theta \qquad (14)$$

Equation (14) states that, near the wall, the convective transport of energy is as important as the conductive transport of heat. Eq. (14) also states that the convective term is proportional to the velocity. As a result, the higher the velocity, the higher the convective term. However, the presence of the wall and the viscosity reduces the velocity inside the thermal boundary layer to zero: $\upsilon_i(\xi_2=0)=0$. Besides, Eq. (13) states that the higher the Prandtl number, the higher the reduction of velocity. It is interesting to study the following limits.

a. Pr tends to infinity. This is the situation for water at 10°C whose Prandtl number is near ten (see Table 1). When the Prandtl number tends to infinity, the viscosity dominates the velocity inside the thermal boundary layer. This result is obtained from retaining in Eq. (13) the last term as the dominant one: $\partial_2 \partial_2 \upsilon_1 = 0 \Rightarrow \upsilon_1 = C\xi_2$. Here C is a constant imposed by the velocity outside of the thermal boundary layer.

b. Pr tends to zero. A negligible Prandtl number produces the higher velocity inside the thermal boundary layer. Although this extreme case is not representative of common fluids, it may be useful for obtaining an upper bound to the maximum heat transfer (Benavides, 2009). This result is obtained from neglecting in Eq. (13) the last term: $\upsilon_1 \partial_1 \upsilon_1 = -\partial_1 p$. The vanishing viscosity allows to approach the velocity near the wall by a parallel flux (i=1) which does not depend on the transversal coordinate (i=2).

The heat transferred over a square region of the wall with an area $L_1 L_3$, which accomplishes $L \gg L_1 \sim L_3 \gg \max(\delta_\mu, \delta_k)$, amounts to:

$$\int_0^{L_1 L_3} -k \frac{\partial T}{\partial x_2}\bigg|_{x_2=0} dx_1 dx_3 = kL_3(T_W - T_L) \int_0^\infty \frac{\partial \theta}{\partial \xi_2}\bigg|_{\xi_2=0} d\xi_1 \qquad (15)$$

When the Prandtl number is near one, such as the Prandtl number of air or water at higher temperatures, the velocity in the thermal boundary layer is neither linear nor constant with the transversal component. In general, Eqs. (13) and (14) must be integrated with the boundary conditions $\theta(\xi_2=0)=\upsilon_i(\xi_2=0)=0$, $\theta(\xi_2\to\infty)=(T_W-T_{ext})/(T_W-T_L)$, and $\upsilon_i(\xi_2\to\infty)=\upsilon_{ext}$ being T_{ext} and υ_{ext} the solution obtained from Eqs. (1), (2) and (9) with Re=∞ and Pe=∞. The condition $\theta(\xi_2\to\infty)=(T_W-T_{ext})/(T_W-T_L)$ indicates that it is convenient to rescale the function θ as $(T_W-T_L)\theta/(T_W-T_{ext})=\theta_b$, which has to accomplish the boundary conditions $\theta_b(\xi_2=0)=0$, $\theta_b(\xi_2\to\infty)=1$. This change of variable does not affect the form of Eqs. (13) and (14) so that the function θ_b only can depend on the Prandtl number and on the value of υ_{ext}. This change of variable allows rewriting the above expression as:

$$\int_0^{L_1L_3} -k\frac{\partial T}{\partial x_2}\bigg|_{x_2=0} dx_1 dx_3 = kL_3(T_W - T_{ext})\int_0^\infty \frac{\partial \theta_b}{\partial \xi_2}\bigg|_{\xi_2=0} d\xi_1 = kL_3(T_W - T_{ext})f(\text{Pr}, \upsilon_{ext}) \qquad (16)$$

Note that, in general, the external solution depends on the position of the surface where the region is located. Although it has been assumed that this dependence is negligible when it is compared with the transversal variation through the boundary layer, it can give a significant contribution when it is evaluated along the full wall. The convective heat transfer coefficient for the full device is defined as:

$$\int_0^{S_W} -k\frac{\partial T}{\partial x_2}\bigg|_{\substack{solid \\ surface}} dS_W = \int_0^{S_W} kf(\text{Pr}, \upsilon_{ext})(T_W - T_{ext})dS_W \qquad (17)$$

It is convenient to introduce a spatial-averaged temperature $T_P(t)$ and a spatial-averaged heat transfer coefficient $h(t)$, by means of the following definition:

$$\int_0^{S_W} kf(\text{Pr}, \upsilon_{ext})(T_W - T_{ext})dS_W = S_W h(t)(T_W - T_P(t)) \qquad (18)$$

Obviously, Eq. (18) states that the heat transfer coefficient depends on the convention used for defining T_P (Baehr & Stephan, 2006). This question is also important for oscillating flows, and hence it has been discussed in the literature (Faghri et al., 1979; Guo & Sung, 1997; Benavides, 2009). Note that Eq. (18) states that the final outcome is given by the product of T_P and h: the heat transfer coefficient is used only as an intermediate function. In section 2.3 (see Eq. 35), the logarithmic mean temperature will be used to model T_P. This assumption will be discussed later. As Eq. (18) indicates, functions $T_P(t)$ and $h(t)$ depend on the Prandtl number, and on the external solution which also depends on the Strouhal number and on the boundary conditions. For oscillating flows, the effect of the pulsation on the velocity near the wall can be described by a temporal evolution of the external solution. This external solution depends both, on the time-averaged mass flow rate and on the oscillatory component of the mass flow rate. It is convenient to define the oscillating component of the mass flow rate as:

$$\frac{G(t)}{\bar{G}} - 1 = \varepsilon g_1(t) + \varepsilon^2 g_2(t) + 0(\varepsilon^3) \qquad (19)$$

where $0 < \varepsilon \ll 1$ is a dimensionless number that assures a weakly oscillating flow, and $g_1(t)$ and $g_2(t)$ are two dimensionless functions taking into account the effects of the oscillation on the mass flow rate. Here, $G(t)$ is the instantaneous mass flow rate and $\bar{G}$ is the stationary mass flow rate. (Through the chapter, a bar above the symbols means stationary solution, i.e., the solution for $\varepsilon=0$.) The stationary mass flow rate $\bar{G}$ induces a heat transfer process which can be obtained from a characteristic velocity U, and a characteristic cross sectional area A, which define a Reynolds number given by the expression:

$$\text{Re} = \frac{\rho LU}{\mu} = \frac{L\bar{G}}{\mu A} \qquad (20)$$

Since the oscillatory part of the mass flow rate modifies the velocities υ_{ext} and the temperatures T_{ext}, it also modifies the heat transfer process. Let $\wp$ be the set of parameters that are necessary to define the function $G/\bar{G}-1$ for any value of time; for example, parameters that might belong to the set $\wp$ are the relative amplitude of the oscillation or its phase. Although parameter ε could belong to set $\wp$, due to its importance, it will be explicitly written as an argument. Thus, in general, the functions $T_P(t)$ and $h(t)$ depend also on Prandtl, Reynolds and Strouhal numbers and on the set of parameters defining the oscillation, i.e., $T_P(t;Pr,Re,St,\wp,\varepsilon)$ and $h(t;Pr,Re,St,\wp,\varepsilon)$. Finding a solution of the heat transfer problem requires a model for both, T_P and h. This will be done in following sections. For weakly oscillating flows, it is $\varepsilon\ll1$ and the effect of the pulsation on the heat transfer coefficient can be described by:

$$h\left(t;\text{Pr},\text{Re},\text{St},\wp,\varepsilon\right)=h\left(t;\text{Pr},\text{Re},\text{St},\wp,0\right)\left[1+h_1\left(t;\text{Pr},\text{Re},\text{St}\right)\varepsilon+h_2\left(t;\text{Pr},\text{Re},\text{St}\right)\varepsilon^2+0\left(\varepsilon^3\right)\right] \quad (21)$$

Finally, we will assume that in absence of oscillation of the mass-flow rate there is not any self-oscillating behaviour, i.e., if $\varepsilon=0$, the solution does not depend on time. Under this condition, the leading term in the above expression is the convective heat transfer coefficient without oscillation, $\bar{h}$. Thus, the above expression can be rewritten as:

$$\frac{h\left(t;\text{Pr},\text{Re},\text{St},\wp,\varepsilon\right)}{\bar{h}\left(\text{Pr},\text{Re}\right)}-1=h_1\left(t;\text{Pr},\text{Re},\text{St},\wp\right)\varepsilon+h_2\left(t;\text{Pr},\text{Re},\text{St},\wp\right)\varepsilon^2+0\left(\varepsilon^3\right) \quad (22)$$

2.2 Estimation of heat transfer coefficient for weakly oscillating flows

For stationary flows the heat transfer coefficient is obtained by relating Nusselt, Reynolds and Prandtl numbers. A frequently used expression for this function is (Baehr & Stephan, 2006):

$$\text{Nu}=K\,\text{Re}^\alpha\,\text{Pr}^\beta \quad (23)$$

where K, α and β are dimensionless constants that depend on the geometry and on the type of flow. Here, the Nusselt number is defined as usual, $\text{Nu}=\bar{h}L/k$, where L is a characteristic length associated with the device geometry and k is the fluid thermal conductivity at the representative temperature in that region. From this expression, we can obtain the heat transfer coefficient for stationary flows as:

$$\bar{h}=\frac{K}{L}\text{Re}^\alpha\,\text{Pr}^\beta \quad (24)$$

Because the Reynolds number depends linearly on the velocity, any variation of the velocity must induce a variation of the heat transfer coefficient. This fact can be used to estimate the value of function h in Eq. (18) by means of $\bar{h}$. The following expression can be used as a first attempt:

$$h\left(t;\text{Pr},\text{Re},\text{St},\wp,\varepsilon\right)\cong\bar{h}\left(\text{Pr},\frac{LG(t;\wp,\varepsilon)}{\mu A}\right)=\bar{h}\left(\text{Pr},\text{Re}+\text{Re}\left(\frac{G(t;\wp,\varepsilon)}{\bar{G}}-1\right)\right) \quad (25)$$

For weakly oscillating flows it is $G/\bar{G}-1 << 1$, and hence, the expression above can be expanded as:

$$
\begin{aligned}
\bar{h}\left(\text{Pr},\text{Re}+\text{Re}\left(\frac{G}{\bar{G}}-1\right)\right) = \\
\bar{h}\left(\text{Pr},\text{Re}\right) + \text{Re}\left.\frac{\partial\bar{h}}{\partial\text{Re}}\right|_{G=\bar{G}}\left(\frac{G}{\bar{G}}-1\right) + \frac{\text{Re}^2}{2}\left.\frac{\partial^2\bar{h}}{\partial\text{Re}^2}\right|_{G=\bar{G}}\left(\frac{G}{\bar{G}}-1\right)^2 + 0\left(\frac{G}{\bar{G}}-1\right)^3
\end{aligned}
\tag{26}
$$

The comparison between Eq. (26) and Eq. (22) allows writing an estimation of h_1 and h_2 as:

$$
h_1\left(t;\text{Pr},\text{Re},\text{St},\wp\right)\varepsilon \cong \frac{\text{Re}}{\bar{h}\left(\text{Pr},\text{Re}\right)}\left.\frac{\partial\bar{h}}{\partial\text{Re}}\right|_{G=\bar{G}}\left(\frac{G(t;\wp,\varepsilon)}{\bar{G}}-1\right)
\tag{27}
$$

$$
h_2\left(t;\text{Pr},\text{Re},\text{St},\wp\right)\varepsilon^2 \cong \frac{\text{Re}^2}{2\bar{h}\left(\text{Pr},\text{Re}\right)}\left.\frac{\partial^2\bar{h}}{\partial\text{Re}^2}\right|_{G=\bar{G}}\left(\frac{G(t;\wp,\varepsilon)}{\bar{G}}-1\right)^2
\tag{28}
$$

From Eq. (24), we can estimate the value of functions h_1 and h_2 in Eq. (21) as:

$$
h_1 \cong \alpha g_1(t;\wp)
\tag{29}
$$

$$
h_2 \cong \alpha g_2(t;\wp) + \frac{\alpha(\alpha-1)}{2}g_1(t;\wp)^2
\tag{30}
$$

This approximation was explored by Benavides (2009) with a reasonable succes for different configurations. For example, one interesting case is the incompressible laminar flow in circular tubes, that assumes all the properties to be constant and both hydrodynamic and thermally fully developed, where it is known (Baehr & Stephan, 2006) that the Nusselt number in this case does not depend on the Reynolds and Prandtl numbers, i.e., $\alpha=\beta=0$. Additionally, it has been shown (Chattopadhyay et al., 2006) that a circular tube in the laminar regime under pulsating flow conditions does not have any oscillation of the local Nusselt number if the flow is both thermally and hydrodynamically developed. The present model explains this behavior: the stationary solution for a constant wall temperature Nu=3.66 (Baehr & Stephan, 2006) shows that in this case α is zero and hence Eqs. (18), (20), (29) and (30) avoid any fluctuation of the heat transfer coefficient. However, Chattopadhyay et al. (2006) also found that the Nusselt number varies in time in the near-entry region of the pipe. The explanation comes again from Eqs. (29) and (30) by taking into account that the thermal entry flow with a fully developed velocity profile has a behavior given by the Léveque solution Nu~Re$^{0.33}$ (Baehr & Stephan, 2006), i.e., $\alpha=0.33$, and hence the expansion given by Eq. (18), together with Eqs. (29) and (30), retains the pulsation effects.

2.3 Integral formulation of the energy conservation for weakly oscillating flows

The model given by Eq. (18) allows calculating the heat transferred if the spatial-averaged temperature T_P and the heat transfer coefficient h are known. The heat transfer coefficient can be estimated by means of Eqs. (22), (24), (29) and (30). This section will introduce the estimation of T_P as a function of time. For this purpose, the physics involved will be

simplified to retain only the most important aspects for the dynamical response. Let us define V as the volume of fluid inside the device where the unsteady temperature field T and the three-dimensional unsteady velocity field u_i are being studied; let be $S(V)$ the surface that limits the volume V. The Reynolds' transport theorem applied to the energy balance leads to:

$$\frac{dQ}{dt} = \int_V \frac{\partial}{\partial t}\left(\rho c T + \rho \sum_{i=1}^{3} \frac{u_i^2}{2}\right) d^3 x + \oint_{S(V)} \left(c T + \frac{P}{\rho} + \sum_{i=1}^{3} \frac{u_i^2}{2}\right)\rho \sum_{i=1}^{3} u_i \cdot dA^i \tag{31}$$

The term on the left-hand side of the equality represents the heat flux and dA is a surface element vector. Since $u_i^2/2cT \ll 1$ holds due to $U^2 \ll U_c^2 < 2cT$ [see Eq. (8) and Tables 1 and 2], the kinetic energy can be neglected when it is compared with the internal energy of the fluid. Additionally, for an ideal gas, which satisfies $P = \rho RT$, the specific heat at constant pressure $c_p = c + R$ appears; for an incompressible flow, the following inequality holds $P/\rho cT \ll 1$ and it can be considered $c_p = c$. These considerations lead to:

$$\frac{dQ}{dt} = \int_V \frac{\partial}{\partial t}(\rho c T) d^3 x + G c_p T_H - G c_p T_L \tag{32}$$

Here, $\rho c_p T_L$ and $\rho c_p T_H$ are the spatial-averaged specific enthalpies (specific internal energies for a liquid) over the inlet and exit ports respectively. If there is not any source of mechanical work in the volume V, the surface $S(V)$ does not change with time and hence the temporal derivative and the spatial integral commutate:

$$\frac{dQ}{dt} = \frac{d}{dt}\int_V \rho c T d^3 x + G c_p T_H - G c_p T_L \tag{33}$$

Although the fluid temperature changes over the device, the integral can be removed by defining $\rho c T_p$ as the spatial-averaged specific internal energy over the volume V, and hence the energy balance equation leads to:

$$\frac{dQ}{dt} = V \frac{d}{dt}\left[\rho c T_P(t)\right] + G c_p \left[T_H - T_L\right] \tag{34}$$

Finally, the spatial-averaged specific internal energy will be modelled by considering that the spatial averaged density does not change over time, and that the spatial-averaged temperature T_p follows the logarithmic mean temperature (Baehr & Stephan, 2006) given by (this assumption will be discussed later):

$$T_P = T_W - \frac{T_H - T_L}{\ln\dfrac{T_W - T_L}{T_W - T_H}} \tag{35}$$

Taking into account Eq. (20), the heat flow amounts to:

$$\frac{dQ}{dt} = h S_W (T_W - T_P) \tag{36}$$

Here h is the spatial-averaged heat transfer coefficient defined by Eqs. (18) and (22), and S_W is the wall area at the temperature T_W. The energy balance comes from Eqs. (34) and (36) with the spatial-averaged temperature defined by Eq. (35):

$$hS_W(T_W - T_P) = \rho V c \frac{dT_P}{dt} + Gc_p(T_H - T_L) \tag{37}$$

The temporal response of the device is obtained by solving Eqs. (35) and (37) for T_P and T_W. For studying the solution, it is convenient to use a dimensionless form of these equations and variables. For this purpose, let us define a dimensionless measure of the heating efficiency as:

$$\eta(T_H) = \frac{T_H - T_L}{T_W - T_L} \tag{38}$$

The dimensionless coefficient that takes into account the temperature inside the device is:

$$\theta(T_P) = \frac{T_W - T_P}{T_W - T_L} \tag{39}$$

The dimensionless coefficient that takes into account the outlet temperature is:

$$\theta(T_H) = \frac{T_W - T_H}{T_W - T_L} = 1 - \eta(T_H) \tag{40}$$

These coefficients transform Eq. (35), which defines the logarithmic temperature, into:

$$\ln\left(1 - \eta(T_H)\right) + \frac{\eta(T_H)}{\theta(T_P)} = 0 \tag{41}$$

and the energy balance into:

$$\frac{h}{\overline{h}}\theta(T_P) + \frac{\rho V c}{\overline{h}S_W}\frac{d\theta(T_P)}{dt} = \frac{\overline{G}c}{\overline{h}S_W}\frac{G}{\overline{G}}\eta(T_H) \tag{42}$$

This differential equation let us define a characteristic time t_c (see Eq. 43) and a characteristic dimensionless number χ (see Eq. 44) which depends on the stationary solution.

$$t_c = \frac{\rho V c}{\overline{h}S_W} \quad ; \quad t = t_c \tau \tag{43}$$

$$\chi = \frac{\overline{h}S_W}{\overline{G}c_p} \tag{44}$$

As a consequence of the above definitions, the behaviour of the device is characterized by the following two dimensionless equations:

$$\ln\left(1 - \eta(T_H(\tau))\right) + \frac{\eta(T_H(\tau))}{\theta(T_P(\tau))} = 0 \tag{45}$$

$$\frac{h(\tau)}{\overline{h}}\theta(T_P(\tau)) + \frac{d\theta(T_P(\tau))}{d\tau} = \frac{1}{\chi}\frac{G(\tau)}{\overline{G}}\eta(T_H(\tau)) \tag{46}$$

2.4 Non-oscillating solution

The condition $\varepsilon=0$ retains only the leading terms of the solution, which can be identified with the stationary part of the problem. Therefore, when we are interested on the stationary solution, Eqs. (45) and (46) admit the following simplification:

$$\ln\left(1-\eta(\overline{T}_H)\right) + \frac{\eta(\overline{T}_H)}{\theta(\overline{T}_P)} = 0 \tag{47}$$

$$\frac{\eta(\overline{T}_H)}{\theta(\overline{T}_P)} = \chi \tag{48}$$

The stationary solution obtained from both equations is:

$$\eta(\overline{T}_H) = 1 - e^{-\chi} \tag{49}$$

$$\theta(\overline{T}_P) = \frac{1-e^{-\chi}}{\chi} \tag{50}$$

$$\theta(\overline{T}_H) = 1 - \eta(\overline{T}_H) = e^{-\chi} \tag{51}$$

For the subsequent discussions, it is convenient to define the dimensionless number Z as:

$$\frac{\theta(\overline{T}_P)}{\theta(\overline{T}_H)} = \frac{1-e^{-\chi}}{\chi e^{-\chi}} = 1 + \frac{1}{Z} \tag{52}$$

$$Z = \frac{\chi e^{-\chi}}{1-(1+\chi)e^{-\chi}} \tag{53}$$

Since it is $Z>0$ for any value of $\chi>0$, the above expressions lead to the following inequalities concerning the temperatures involved: $T_L < \overline{T}_P < \overline{T}_H < T_W$.

2.5 Second-order expansion of the oscillating solution

The stationary solution found in the previous section allows rewriting Eqs. (45) and (46) in the following form:

$$\ln\left(1 - \frac{\eta(T_H(\tau))}{\eta(\overline{T}_H)}(1-e^{-\chi})\right) + \frac{\eta(T_H(\tau))}{\eta(\overline{T}_H)}\frac{\theta(\overline{T}_P)}{\theta(T_P(\tau))}\chi = 0 \tag{54}$$

$$\frac{h(\tau)}{\overline{h}}\frac{\theta(T_P(\tau))}{\theta(\overline{T}_P)} + \frac{d}{d\tau}\frac{\theta(T_P(\tau))}{\theta(\overline{T}_P)} = \frac{G(\tau)}{\overline{G}}\frac{\eta(T_H(\tau))}{\eta(\overline{T}_H)} \tag{55}$$

In order to solve these equations, it is necessary to know $G/\overline{G}$ and $h/\overline{h}$. Here, we will use the model for weakly oscillating flows introduced in Section 2.1 as:

$$\frac{G}{\overline{\overline{G}}} = 1 + g_1 \varepsilon + g_2 \varepsilon^2 + 0(\varepsilon^3) \tag{56}$$

$$\frac{h}{\overline{\overline{h}}} = 1 + h_1 \varepsilon + h_2 \varepsilon^2 + 0(\varepsilon^3) \tag{57}$$

The oscillatory solution can be expanded as a series of the small parameter ε as:

$$\frac{\theta(T_P)}{\theta(\overline{\overline{T}}_P)} = 1 + p\varepsilon + q\varepsilon^2 + 0(\varepsilon^3) \tag{58}$$

$$\frac{\eta(T_H)}{\eta(\overline{\overline{T}}_H)} = 1 + r\varepsilon + s\varepsilon^2 + 0(\varepsilon^3) \tag{59}$$

where p, q, r, and s can be found by substituting expressions (56) to (59) in Eqs. (54) and (55). The first and second order terms of these equations lead to:

$$p = -\frac{r}{Z} \tag{60}$$

$$q = -Y\frac{r^2}{Z^2} - \frac{s}{Z} \tag{61}$$

$$\frac{dp}{d\tau} = r - p + g_1 - h_1 \tag{62}$$

$$\frac{dq}{d\tau} = s - q + g_1 r - h_1 p + g_2 - h_2 \tag{63}$$

$$Y = \frac{(2 + \chi)e^{-2\chi} - 4e^{-\chi} + 2 - \chi}{2\left[1 - (1 + \chi)e^{-\chi}\right]^2} \tag{64}$$

Therefore, when the fluctuation is taken into account, the ratio (58) is expressed as:

$$\frac{\theta(T_P)}{\theta(\overline{\overline{T}}_P)} = 1 - \frac{r}{Z}\varepsilon - \left(Y\frac{r^2}{Z^2} + \frac{s}{Z}\right)\varepsilon^2 + 0(\varepsilon^3) \tag{65}$$

The substitution of p and q, given by Eqs. (60) and (61), in Eqs. (62) and (63) yields to:

$$\frac{dr}{d\tau} + (Z + 1)r = Z(h_1 - g_1) \tag{66}$$

$$\frac{ds}{d\tau} + (Z + 1)s = \left(2 + \frac{1}{Z}\right)Yr^2 - (Z - 2Y)g_1 r - (1 + 2Y)h_1 r + Z(h_2 - g_2) \tag{67}$$

This system of differential equations determines r and s when functions g_1, g_2, h_1, and h_2 are given as data. From Eqs. (60) and (61) functions p and q are also determined. Without any

loss of generality for the purpose of the paper, g_1, h_1, p, q, r and s, are oscillating functions that accomplishes:

$$\int_0^{\frac{2\pi}{\omega t_c}} g_1 d\tau = \int_0^{\frac{2\pi}{\omega t_c}} h_1 d\tau = 0 \tag{68}$$

$$\int_0^{\frac{2\pi}{\omega t_c}} \frac{dp}{d\tau} d\tau = \int_0^{\frac{2\pi}{\omega t_c}} \frac{dq}{d\tau} d\tau = \int_0^{\frac{2\pi}{\omega t_c}} \frac{dr}{d\tau} d\tau = \int_0^{\frac{2\pi}{\omega t_c}} \frac{ds}{d\tau} d\tau = 0 \tag{69}$$

As a consequence, Eq. (66) states that the mean value of function r is zero:

$$\int_0^{\frac{2\pi}{\omega t_c}} r d\tau = 0 \tag{70}$$

Contrarily, the term $g_1{}^2$ in Eq. (30) shows that the mean value of function h_2 can be distinct of zero:

$$\int_0^{\frac{2\pi}{\omega t_c}} h_2 d\tau \neq 0 \tag{71}$$

Therefore, function s exhibits a mean value given by Eq. (67) as:

$$\int_0^{\frac{2\pi}{\omega t_c}} s d\tau = \frac{2Z+1}{Z(Z+1)} Y \int_0^{\frac{2\pi}{\omega t_c}} r^2 d\tau - \frac{Z-2Y}{Z+1} \int_0^{\frac{2\pi}{\omega t_c}} g_1 r d\tau - \frac{1+2Y}{Z+1} \int_0^{\frac{2\pi}{\omega t_c}} h_1 r d\tau + \frac{Z}{Z+1} \int_0^{\frac{2\pi}{\omega t_c}} (h_2 - g_2) d\tau \tag{72}$$

Multiplying Eq. (66) by r and taking the mean value of the resulting expression allow expressing the mean value of r^2 as a function of the mean value of $g_1 r$ and $h_1 r$ as:

$$\int_0^{\frac{2\pi}{\omega t_c}} r^2 d\tau = \frac{Z}{Z+1} \int_0^{\frac{2\pi}{\omega t_c}} (h_1 - g_1) r d\tau \tag{73}$$

Thus, Eq. (72) simplifies to:

$$\int_0^{\frac{2\pi}{\omega t_c}} s d\tau = -\frac{Z(Z+1) - Y}{(Z+1)^2} \int_0^{\frac{2\pi}{\omega t_c}} g_1 r d\tau - \frac{Z+Y+1}{(Z+1)^2} \int_0^{\frac{2\pi}{\omega t_c}} h_1 r d\tau + \frac{Z}{Z+1} \int_0^{\frac{2\pi}{\omega t_c}} (h_2 - g_2) d\tau \tag{74}$$

This interesting result shows that the oscillation can modify the time-averaged value of the outlet temperature. Thus, it is plausible to expect that a thermocouple placed on the outlet stream measures this deviation. This solution also shows that this effect is of order ε^2. However, although the time-averaged outlet temperature is related to the heat flux, they are not exactly the same. The heat transferred per unit of time is obtained from Eq. (34) as:

$$\frac{dQ}{dt} = \rho c V \frac{dT_P}{dt} + G c_p (T_H - T_L) \tag{75}$$

The dimensionless form of this equation is:

$$\frac{\dfrac{dQ}{dt}}{\overline{h} S_W (T_W - \overline{\overline{T}}_P)} = -\frac{d}{d\tau} \frac{\theta(T_P)}{\theta(\overline{T}_P)} + \frac{G}{\overline{G}} \frac{\eta(T_H)}{\eta(\overline{T}_H)} \tag{76}$$

The solution given by Eqs. (56) to (59) leads to:

$$\frac{\dfrac{dQ}{dt}}{\overline{h} S_W (T_W - \overline{\overline{T}}_P)} = 1 + \left(r + g_1 - \frac{dp}{d\tau} \right)\varepsilon + \left(s + g_1 r + g_2 - \frac{dq}{d\tau} \right)\varepsilon^2 \tag{77}$$

Remembering Eqs. (68) to (70), the time-averaged flux of heat evolves to:

$$\frac{\omega t_c}{2\pi} \int_0^{\frac{2\pi}{\omega t_c}} \frac{dQ/dt}{\overline{h} S_W (T_W - \overline{\overline{T}}_P)} d\tau - 1 = \varepsilon^2 \frac{\omega t_c}{2\pi} \int_0^{\frac{2\pi}{\omega t_c}} \left(s + g_1 r + g_2 \right) d\tau \tag{78}$$

This expression shows that the terms $g_1 r$ and g_2 under the second integral of Eq. (78) introduce a bias respect to the time-averaged outlet temperature. The solution given by Eq. (74) lets us write the right-hand side of this equation as:

$$\int_0^{\frac{2\pi}{\omega t_c}} \left(s + g_1 r + g_2 \right) d\tau = \frac{Z + Y + 1}{(Z+1)^2} \int_0^{\frac{2\pi}{\omega t_c}} (g_1 - h_1) r \, d\tau + \frac{Z}{Z+1} \int_0^{\frac{2\pi}{\omega t_c}} h_2 \, d\tau + \frac{1}{Z+1} \int_0^{\frac{2\pi}{\omega t_c}} g_2 \, d\tau \tag{79}$$

Equations (74) and (79) differ only in the coefficients that precede the integrals on the right-hand side of both equations. The value of g_1-h_1 can be obtained from Eq. (73), what simplifies the above expression to:

$$\int_0^{\frac{2\pi}{\omega t_c}} \left(s + g_1 r + g_2 \right) d\tau = -\frac{Z + Y + 1}{Z(Z+1)} \int_0^{\frac{2\pi}{\omega t_c}} r^2 \, d\tau + \frac{Z}{Z+1} \int_0^{\frac{2\pi}{\omega t_c}} h_2 \, d\tau + \frac{1}{Z+1} \int_0^{\frac{2\pi}{\omega t_c}} g_2 \, d\tau \tag{80}$$

3. Discussion

In the discussion carried out by Benavides (2009), in order to overcome the problems derived from how the time-averaged temperature is defined (Guo & Suang, 1997), the heat flux was estimated as the time-averaged increment of the specific enthalpy along the device, i.e., as the value of s. Although, this approximation is interesting because the time-averaged outlet temperature is near the one that a thermocouple would measure in the exit port of an experimental arrangement, Eq. (78) shows that the constant part of s is not equivalent to the time-averaged heat flux under oscillating conditions. Indeed, the presence of the term $g_1 r$ modifies averaged value and hence, it also modifies the prediction that the model produces.

Equation (80), which takes into account this term, shows that this term removes completely the possibility of having an enhancement of the heat flux due to the first order terms g_1 and h_1 because the first term on the right-hand side of this equation is always negative. Depending on the sign of the integrals of h_2 and g_2, the heat transfer could suffer enhancement or deterioration. However, note that following the estimation given by Eq. (30) this term is proportional to $\alpha(\alpha-1)/2$, which depends on the level of turbulence in the device and which is maximum for $\alpha=1/2$ (i.e., for laminar flow), proportional to $Z/(Z+1)$ which is maximum for $\chi \rightarrow 0$ (i.e., for low efficiency devices – see the asymptotic behaviour of function Z in Table 4 at the end of Section 3), and proportional to the mean value of g_1^2, which is ½ for a sine law of maximum amplitude without reversing flow. Therefore, the maximum attainable discouragement predicted by this term is near $\alpha(\alpha-1)/4<1/16\sim6\%$. The other term that can produce deterioration is the one with the time-averaged value of g_2, which produces deterioration of heat transfer in the presence of pulsating flow if the pulsation significantly increments the losses through the channel (Kim and Kang, 1998, reported that, in a 2D channel with two heated blocks working with a pulsating flow of air, the force over the blocks is typically amplified by the pulsating flow; the amplitude of the instantaneous friction factor increases dramatically, easily reaching 50 times the stationary value). Nevertheless, this term is proportional to $1/(Z+1)$ which tends to zero when $\chi \rightarrow 0$ and hence it becomes negligible in this limit. It is interesting to note that the limit $\chi \rightarrow 0$ can also be obtained by substituting the logarithmic definition of the averaged temperature [see Eq. (35)] by the condition $T_P=T_L$ (i.e., by $\theta(T_P)=1$). The solution for this definition of the spatial-averaged temperature inside the device comes from substituting Eq. (55) with $\theta(T_P)/\theta(\bar{T}_P)=1$ and hence, the solution is $Z=\infty$, $Y=0$, $p=q=0$, $r=h_1-g_1$, $s=g_1^2-g_1h_1+h_2-g_2$ and $s+g_1r+g_2=h_2$. The last expression shows that the dominant term is the one generated by the second order term of the heat transfer coefficient. Thus, in this limit, the enhancement of the heat transfer requires a positive value of h_2 which is incompatible with the estimation given by Eq. (30), what shows that this estimation has a restricted range of validity. Eq. (35) can also be substituted by $T_P=T_H$ (i.e., by $\theta(T_P)+\eta(T_H)=1$). In this case Eq. (54) must be substituted by $\theta(T_P)/\theta(\bar{T}_P)+\chi\eta(T_H)/\eta(\bar{T}_H)=1+\chi$ and the entire solution remains valid for $Z=1/\chi$ and $Y=0$. It is possible to see that the behaviour of this approach is qualitatively equal to the obtained with the logarithmic definition. Indeed, depending on the chosen values of Z and Y, the solutions in Eqs. (74) and (80) are valid for different definitions of the spatial-averaged temperature T_P. This holds while the relationship between temperatures remains algebraic, which means that the response of both temperatures to the external mass flow rate pulsation is instantaneous. A more detailed model would need a differential equation where the relationship between temperatures included temporal delays; then, the expected solution would depend not only on the value of r^2 but on the value of g_1r and h_1r. Note that Eq. (74) retains these terms for the time-averaged outlet temperature. The approach in the next section is based on retaining only one fundamental harmonic and shows that the outlet temperature may suffer an enhancement when the relative phases between g_1, h_1 and r are correctly chosen.

3.1 Single-harmonic approach

Let us characterise the oscillation by means of only one harmonic. Thus the solution can be written in the following way:

$$g_1 = \frac{g_{1+}e^{j\omega t_c \tau} + g_{1-}e^{-j\omega t_c \tau}}{2} \tag{81}$$

$$h_1 = \frac{h_{1+}e^{j\omega t_c \tau} + h_{1-}e^{-j\omega t_c \tau}}{2} \tag{82}$$

$$r = \frac{r_+ e^{j\omega t_c \tau} + r_- e^{-j\omega t_c \tau}}{2} \tag{83}$$

where subscripts + and – indicates two conjugate complex functions that do not depend on time, and j is the imaginary unit. Then, the solution is obtained from Eqs. (66) and (74) as:

$$r_+ = \frac{Z}{Z+1+j\omega t_c}(h_{1+} - g_{1+}) \tag{84}$$

$$\frac{\omega t_c}{2\pi}\int_0^{\frac{2\pi}{\omega t_c}} s d\tau = -\frac{Z(Z+1)-Y}{(Z+1)^2}\frac{g_{1+}r_- + g_{1-}r_+}{4} - \frac{Z+Y+1}{(Z+1)^2}\frac{h_{1+}r_- + h_{1-}r_+}{4}$$

$$+ \frac{Z}{Z+1}\frac{\omega t_c}{2\pi}\int_0^{\frac{2\pi}{\omega t_c}}(h_2 - g_2)d\tau \tag{85}$$

When Eq. (84) is used to eliminate the function r in Eq. (85), the final solution for the mean value of s arises as:

$$\frac{\omega t_c}{2\pi}\int_0^{\frac{2\pi}{\omega t_c}} s d\tau = \left[-C_1|h_{1+}|^2 + C_2|g_{1+}|^2 - C_3|h_{1+}||g_{1+}|\cos\left(\varphi_{h_{1+}} - \varphi_{g_{1+}}\right)\right]\frac{1}{1+\left(\frac{\omega t_c}{Z+1}\right)^2}$$

$$- C_4|h_{1+}||g_{1+}|\sin\left(\varphi_{h_{1+}} - \varphi_{g_{1+}}\right)\frac{\frac{\omega t_c}{Z+1}}{1+\left(\frac{\omega t_c}{Z+1}\right)^2} + 2C_4\frac{\omega t_c}{2\pi}\int_0^{\frac{2\pi}{\omega t_c}}(h_2 - g_2)d\tau \tag{86}$$

$$C_1 = \frac{Z(Z+Y+1)}{2(Z+1)^3} \quad C_2 = \frac{Z^2(Z+1)-YZ}{2(Z+1)^3} \quad C_3 = C_2 - C_1 \quad C_4 = C_2 + C_1$$

From Eq. (79), the heat transferred amounts to:

$$\frac{\omega t_c}{2\pi}\int_0^{\frac{2\pi}{\omega t_c}}(s + g_1 r + g_2)d\tau = -C_1\frac{1}{1+\left(\frac{\omega t_c}{Z+1}\right)^2}\left[|h_{1+}|^2 + |g_{1+}|^2 - 2|h_{1+}||g_{1+}|\cos\left(\varphi_{h_{1+}} - \varphi_{g_{1+}}\right)\right]$$

$$+ 2C_4\frac{\omega t_c}{2\pi}\int_0^{\frac{2\pi}{\omega t_c}} h_2 d\tau + \frac{1}{Z+1}\frac{\omega t_c}{2\pi}\int_0^{\frac{2\pi}{\omega t_c}} g_2 d\tau \tag{87}$$

3.2 Predicted dependence on the Strouhal number

Expression (86) shows that the time-averaged outlet temperature depends explicitly on the angular frequency as:

$$F = \frac{\Gamma_0 + \Gamma_1 \dfrac{\omega t_c}{Z+1} + \Gamma_2 \left(\dfrac{\omega t_c}{Z+1}\right)^2}{1 + \left(\dfrac{\omega t_c}{Z+1}\right)^2} \tag{88}$$

Here, Γ_0, Γ_1, and Γ_2 are functions that can be obtained from comparing Eqs. (88) and (86). Since these functions depend on the value adopted for h_{1+} and h_2, Eq. (21) states that these functions depend also on the Strouhal number. Note that the Strouhal number and the angular frequency are related to each other by means of the following expression:

$$\text{St} = \frac{\omega L}{U} = \frac{\omega \rho L A}{\bar{G}} = \omega t_c \chi \frac{LA}{V} \frac{c_p}{c} \tag{89}$$

Therefore, function F in Eq. (88) has an implicit dependence on the Strouhal number due to the coefficients Γ_0, Γ_1, and Γ_2, and an explicit dependence due to ω. The influence of the Strouhal number on the coefficients Γ_0, Γ_1, and Γ_2 comes through the effect that produces on the external solution previously discussed in section 2.1. Therefore, in those devices where the external solution does not suffer a significant change due to the variations of the Strouhal number, these coefficients can be considered constant values. In this case, Eq. (89) allows us to rewrite expression (88) as a function that depends on the Strouhal number and on four constants A, B, C and D:

$$F = \frac{A + B\,\text{St} + C\,\text{St}^2}{1 + D\,\text{St}^2} \tag{90}$$

This function does not exhibit any resonant behaviour since all the terms in the denominator are always positive quantities. However, this function presents an extreme at the angular frequency:

$$\frac{\omega t_c}{Z+1} = \frac{\Gamma_2 - \Gamma_0}{\Gamma_1} \pm \sqrt{\left(\frac{\Gamma_2 - \Gamma_0}{\Gamma_1}\right)^2 + 1} \quad \text{or} \quad \text{St} = \frac{C}{BD} - \frac{A}{B} \pm \sqrt{\left(\frac{C}{BD} - \frac{A}{B}\right)^2 + \frac{1}{D}} \tag{91}$$

Since this extreme disappears for those devices where Γ_1 vanishes, the above expression is able to reproduce all the results found in the current scientific literature. For example, for very low frequencies, Eq. (90) can produce the enhancement or deterioration depending on the sign of the coefficient Γ_0 which changes, for example, with the relative phase between the dimensionless heat transfer coefficient, h_1, and the dimensionless mass flow rate coefficient g_1. The same can happen at very high frequencies depending on the sign of Γ_2. Thus, although this expression has been obtained under the assumption of several restrictive hypotheses, it retains an influence on the Strouhal number that reflects the actual behaviour of some heat exchangers. For example, a backward facing step like the one presented in Fig. 1 exhibits a heat transfer enhancement, which was calculated by Velazquez et al. (2007) for several Strouhal

numbers. For this configuration, they reported that the maximum heat transfer is 42% higher than in the steady case. The method of least square allows fitting the simplified model in Eq. (90) giving the following values for the four constants: $A=0$, $B=0.8453$, $C=0.1997$ and $D=1.561$. (The constant $A=0$ imposes that the solution at zero frequency must coincide with the steady one.) The result of the fitting and the numerical data are plotted in Fig. 2. Discrepancies between the numerical calculations and the approach given in this section can be due to the neglected terms, to the harmonics of order greater than one which could be present, and to the fact of having neglected the influence of the Strouhal number on the amplitudes and phases that drive the coefficients A, B and C. Extended discussions about the estimation of these coefficients from physical considerations and about the behaviour of other configurations are given by Benavides (2009).
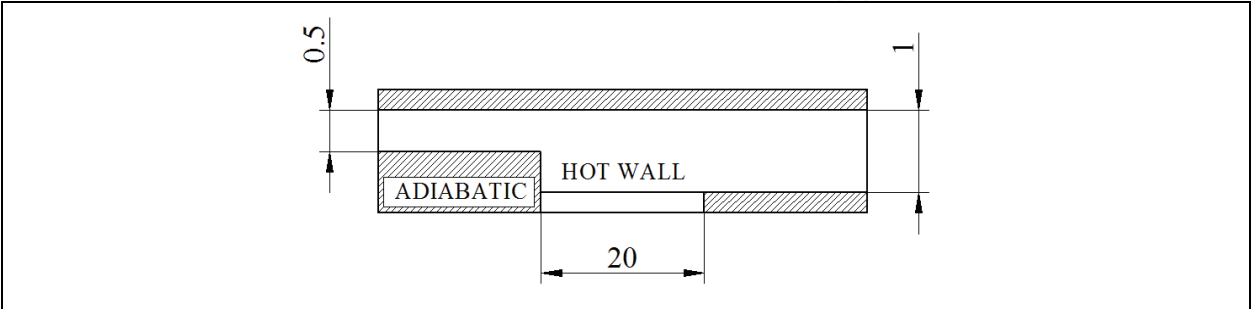
Fig. 1. Dimensionless definition of the 2-D backwards facing step (not at scale). The outlet height of this device is $L=450$ μm. It works with ideal water ($k=0.598$ W K^{-1}m^{-1}, $\mu=10^{-3}$ Pa s, $c=4180$ J kg^{-1}K^{-1} and $\rho=998$ kg m^{-3}) in an operational point identified by Nu=5.18 and Re=100. These values give the following non-dimensional characterization of the stationary heat flow: $\chi=0.074$, $\eta(\overline{T}_H)=0.071$, $\theta(\overline{T}_P)=0.96$, $Z=26$ and $Y=0.34$.
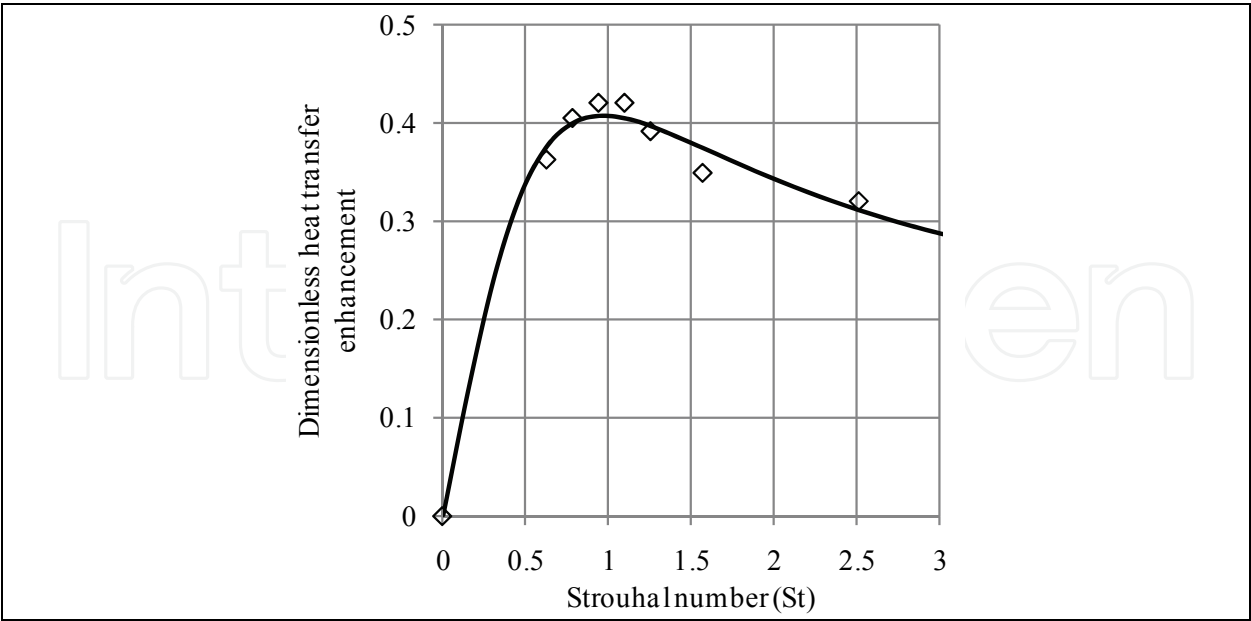

Fig. 2. Set of data points (diamond points) obtained from direct numerical simulation (Velazquez et al., 2007) for different values of the frequency for the device whose scheme is given in Fig. 1. The result of fitting these data points with the model given by Eq. (90) (solid line) gives $A=0$, $B=0.8453$, $C=0.1997$ and $D=1.561$.

Equation (87) can also be represented by Eq. (88). However, for this equation, $\Gamma_1=0$ always holds. This means that the result expressed by Eq. (87) does not have extremes. Besides, the condition $\Gamma_0=0$ removes any effect at zero frequency. Finally, in case of considering Γ_2 constant with the frequency, the model would follow the expression:

$$F = \frac{C\mathrm{St}^2}{1+D\mathrm{St}^2} \qquad (92)$$

Figure 3 presents a qualitative drawing of Eqs. (90) and (92). Note that the condition $\Gamma_0=0$ must only be satisfied for zero frequency. Besides, as it has been discussed above, one possible reason for losing the term proportional to Γ_1 is the algebraic relationship for defining the spatial-averaged temperature. Therefore, Eq. (92) is a very restrictive case of Eq. (90). Besides, coefficients in Eqs. (90) and (92) should depend on Strouhal number with a mathematical law fixed by the device geometry; since Eq. (90) has more degrees of freedom that Eq. (90) it will be a better choice for fitting empirical laws derived from different test configurations. Note that, due to the inertial terms, it is plausible to expect a negligible response for higher frequencies: this feature is not described by Eq. (90) except for the case $C=0$. Since the constant C is required to model a flat asymptotic behaviour for high Strouhal numbers, an external model to characterize the dependency of the coefficients A, B and C is required. The correction due to this missing model is qualitatively represented as the dashed lines of Fig. 3.
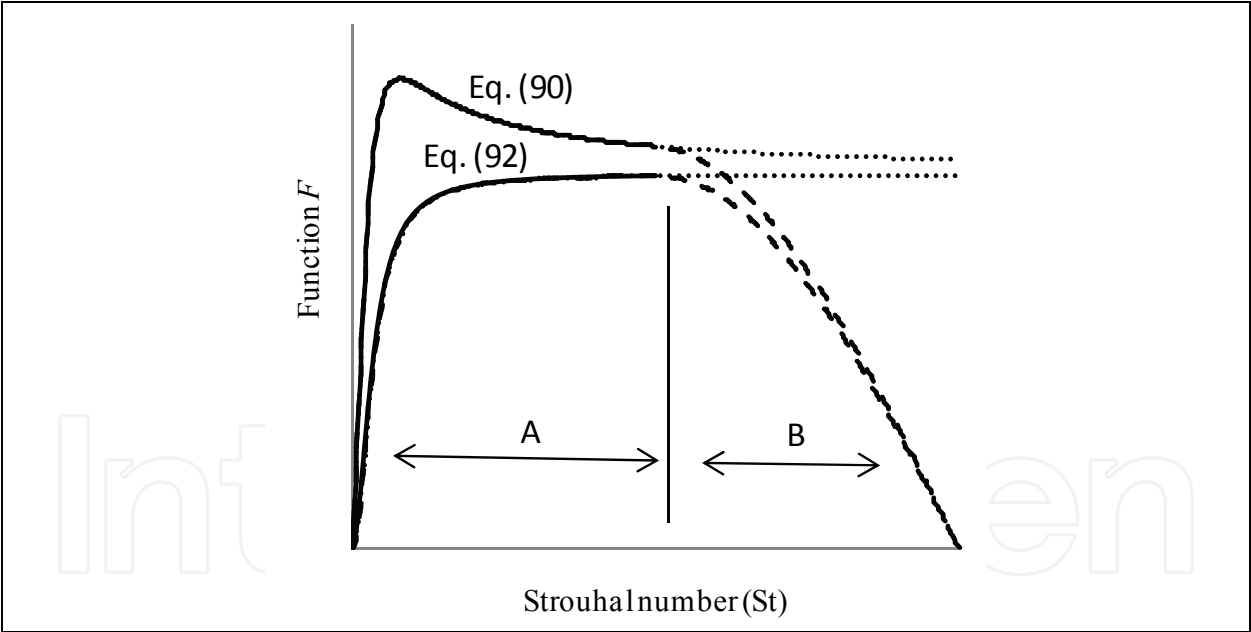

Fig. 3. Solid and dot curves are the solutions obtained from Eqs. (90) (upper line) and (92) with the same values of constants A, B, C and D (this qualitative drawing can be reproduced by choosing the values 0, 0.8, 0.5 and 0.5 for A, B, C and D). In the range of low Strouhal numbers, labelled as region A in the figure, it is assumed that constants A, B, C and D do not depend on the Strouhal number; in the region of higher Strouhal numbers, labelled as region B, the effect of the Strouhal number on the constants could be significant, and hence dot curves represents the behaviour predicted by the model for high Strouhal numbers while dashed curves represents the plausible decay due to the variation of constants A, B, C and D with the Strouhal number.

As expected, the model does not predict any change respect to the steady state when χ tends to infinity. The proof of this statement comes from the asymptotic behaviour of the coefficients C_1, C_2, C_3 and C_4, that tends to zero exponentially when χ tends to infinity. The situation described by $\chi \to \infty$ represents a very effective device where the steady heat transfer coefficient is so high that the outlet temperature matches the hottest wall temperature. Therefore, the enhancement predicted by this model cannot be obtained for those devices whose efficiency is high or, in other words, the enhancement only is present for low efficiency devices. Normally, actual devices have small values of χ, typically $\chi < 0.1$, and hence the efficiency $\eta(\overline{T}_H)$ of the device is close to zero. The asymptotic behaviour of the relevant functions and coefficients for both limits, low and high values of χ, are collected in Table 4.

$\eta(\overline{T}_H) = 1 - e^{-\chi}$	$\chi - \dfrac{\chi^2}{2} + 0(\chi^3) << 1$	$0(1)$
$\theta(\overline{T}_P) = \dfrac{1 - e^{-\chi}}{\chi}$	$1 - \dfrac{\chi}{2} + \dfrac{\chi^2}{6} + 0(\chi^3) < 1$	$0\left(\dfrac{1}{\chi}\right)$
$\theta(\overline{T}_H) = e^{-\chi}$	$1 - \chi + \dfrac{\chi^2}{2} + 0(\chi^3) < 1$	$0\left(\dfrac{1}{e^\chi}\right)$
$\dfrac{\theta(\overline{T}_P)}{\theta(\overline{T}_H)} = 1 + \dfrac{1}{Z} = \dfrac{1 - e^{-\chi}}{\chi e^{-\chi}}$	$1 + \dfrac{\chi}{2} + \dfrac{\chi^2}{6} + 0(\chi^3) > 1$	$0\left(\dfrac{e^\chi}{\chi}\right)$
$Z = \dfrac{\chi e^{-\chi}}{1 - (1 + \chi)e^{-\chi}}$	$\dfrac{2}{\chi} - \dfrac{2}{3} + \dfrac{\chi}{18} + \dfrac{\chi^2}{270} + 0(\chi^3) >> 1$	$0\left(\dfrac{\chi}{e^\chi}\right)$
$Y = \dfrac{(2 + \chi)e^{-2\chi} - 4e^{-\chi} + 2 - \chi}{2\left[1 - (1 + \chi)e^{-\chi}\right]^2}$	$\dfrac{1}{3} + \dfrac{\chi}{9} + \dfrac{\chi^2}{45} + 0(\chi^3)$	$0(\chi)$
$C_1 = \dfrac{Z(Z + Y + 1)}{2(Z + 1)^3}$	$\dfrac{\chi}{4} - \dfrac{\chi^2}{8} + 0(\chi^3)$	$0\left(\dfrac{\chi^2}{e^\chi}\right)$
$C_2 = \dfrac{Z^2(Z + 1) - ZY}{2(Z + 1)^3}$	$\dfrac{1}{2} - \dfrac{\chi}{2} + \dfrac{\chi^2}{6} + 0(\chi^3)$	$0\left(\dfrac{\chi^2}{e^\chi}\right)$
$C_3 = \dfrac{Z^3 - Z(2Y + 1)}{2(Z + 1)^3}$	$\dfrac{1}{2} - \dfrac{3}{4}\chi + \dfrac{7}{24}\chi^2 + 0(\chi^3)$	$0\left(\dfrac{\chi^2}{e^\chi}\right)$
$C_4 = \dfrac{Z}{2(Z + 1)}$	$\dfrac{1}{2} - \dfrac{\chi}{4} + \dfrac{\chi^2}{24} + 0(\chi^3)$	$0\left(\dfrac{\chi}{e^\chi}\right)$

Table 4. Limits of the relevant functions and constants for $\chi \to 0$ and $\chi \to \infty$.

Finally, the model predicts that the form of measuring the heat flux is completely decisive when oscillating flows are present: in Eq. (90), which is a simplification of Eq. (86), the heat flux is obtained from averaging the outlet temperature or the specific enthalpy; in Eq. (92), which is a simplification of Eq. (87), it is obtained from averaging the enthalpy. As explained, both descriptions lead to the difference between the solid lines in region A of Fig. 3. While the averaged outlet temperature is closer to the response of a thermocouple placed

in the outlet flow, the determination of the heat flux requires two time recordings: the model described by Eqs. (78) and (87) shows that the measurement setup should include the instantaneous value of the temperature and the instantaneous value of the mass flow rate. For this reason, in an experimental setup where the heat flux in the wall is only measured by a time-averaged value obtained from a final thermocouple, the heat transfer enhancement of the device could be overestimated. For example, for $\chi \to 0$, coefficients C_1, C_2, C_3 and C_4 tend to 0, ½, ½, ½ respectively, this means that the model predicts a response of order unity for the three terms involving St^0, St and St^2 in the outlet temperature given by Eq. (86) whereas the only term of order unity in Eq. (87) is the one associated to St^0.

4. Conclusion

The proposed model applies to channels with different solid structures on the inside under the assumptions: *i*) the amplitude of the oscillation of the mass flow rate is small when it is compared with the averaged mass flow rate; *ii*) the spatial-averaged temperature inside the device and the outlet temperature are related to each other by means of an algebraic equation; *iii*) there is only one dominant harmonic; and *iv*) the effect of the Strouhal number on the coefficients that determine the expansions is negligible. The work shows that, under these assumptions, the outlet temperature is determined as a function of the frequency of the oscillation. This dependence on the Strouhal number is characterised by the ratio of two polynomials of second order where the linear term of the polynomial in the denominator does not appears. As a consequence, the time-averaged outlet temperature can exhibit a maximum response for a Strouhal number determined by the model. The model also predicts that, under the aforementioned assumptions, the time-averaged heat flux does not exhibit such a maximum; however, it is suggested that this feature probably is due to the assumption *ii*) that inhibits any temporal delay between temperatures. Besides, such as the derivation of the model establishes, the coefficients that determine the expansion depend on the Strouhal number: this implies that the model fixed by the ratio of two polynomials should be modified. The greater the effects of the Strouhal number on the coefficients, the greater the discrepancies. In particular, it has been discussed that due to the inertial terms, it is plausible to expect that the coefficients tend to zero for high Strouhal numbers, and hence the heat transfer enhancement will tend to zero when the Strouhal number tends to infinity. This fact introduces an effect highly dependent on the device geometry and produces a maximum response for a given Strouhal number that cannot be calculated with the present model. The relative importance of these two physical phenomena establishes the final response for a given device. However, it has been shown that the formula obtained from the model fits well the numerical results obtained for a 2-D backward facing step with the hot surface parallel to the flow in an adiabatic channel. Thus, the presented model reveals a mathematical law that can be used to fit several empirical results and to collect them under a similar dimensionless law. A final important conclusion is that those testing procedures where the heat flux is estimated by a time-averaged measurement of the outlet temperature might overestimate the heat transfer enhancement. A full characterization of the heat transfer requires recording the temporal evolution of both, the outlet temperature and the mass flow rate. Further studies are required to remove assumption *ii*), which imposes severe limitations to the results, and to incorporate the effect of the external solution on the dimensionless coefficients, which are very sensitive to the geometry and to the flow patterns in the channel, especially when stagnant or recirculation regions are involved.

5. References

Backhaus, S. & Swift, G.W. (2000). A thermoacoustic-Stirling heat engine: Detailed study, *J. Acoust. Soc. Am.*, Vol. 107, No. 6, (June 2000) (3148-3166), ISSN

Baehr, H. D. & Stephan, K. (2006). *Heat and Mass Transfer*, Springer-Verlag Berlin Heidelberg

Benavides, E.M. (2006). An analytical model of self-starting thermoacoustic engines, *Journal of Applied Physics*, Vol. 99 (2006)

Benavides, E.M. (2007). Thermoacoustic nanotechnology: Derivation of a lower limit to the minimum reachable size, *Journal of Applied Physics*, Vol. 101, No. (2007)

Benavides, E.M. (2009). Heat Transfer Enhancement by Using Pulsating Flows, *Journal of Applied Physics*, Vol. 101, No. (2007)

Chattopadhyay, H.; Durst, F. & Ray, S. (2006). Analysis of heat transfer in simultaneously developing pulsating laminar flow in a pipe with constant wall temperature, *Int. Commun Heat Mass Transfer*, Vol. 33 (2006) (475-481)

Cho, H.W. & Hyun, J.M. (1990). Numerical solution of pulsating flow and heat transfer characteristic in a pipe, *Int. J. Heat Flow*, Vol. 11, No. 4 (1990) (321-330)

Faghri, M.; Javadani, K. & Faghri, A. (1979). Heat Transfer with laminar pulsating flow in a pipe, *Lett. Heat Mass Transfer* , Vol. 6 (1979) (259-270)

Gardner, D.L. & Swift, G.W. (2003). A cascade thermoacoustic engine, *J. Acoust. Soc. Am.*, Vol. 114, No. 4, (October 2003), (1905-1919)

Guo, Z. & Sung, H.J. (1997). Analysis of the Nusselt number in pulsating pipe flow, *Int. J. Heat Mass Transfer*, Vol. 40, No. 10 (1997) (2486-2489)

Harvey, A.P.; Mackley, M.R. & Seliger, T. (2003). Process intensification of biodiesel production using a continuous oscillatory flow reactor, *Journal of Chemical Technology & Biotechnology*, Vol. 78, No. 2-3 (2003) (338-341)

Hemida, H. N.; Sabry, M.N.; Abdel-Rahim, A. & Mansour, H. (2002). Theoretical analysis of heat transfer in laminar pulsating flow, *Int. J. Heat Mass Transfer*, Vol. 45 (2002) (1767-1780)

Kim, S.Y. & Kang, B.H. Forced convection heat transfer from two heated blocks in pulsating channel flow, *Int. J. Heat Mass Transfer*, Vol 41, No.3 (1998) (625-634)

Lee, C.T.; Mackley, M.R.; Stonestreet, P. & Middelberg, A.P.J. (2001). Protein refolding in an oscillatory flow reactor, *Biotechnology Letters*, Vol. 23, No. 22 (2001) (1899-1901)

Lide, D.R. (2004). *CRC handbook of chemistry and physics: a ready-reference book of chemical and physical data : 2004-2005*, CRC Press Boca Raton, ISBN, Florida

Mackley, M.R. & Stonestreet, P. (1995). Heat transfer and associated energy dissipation for oscillatory flow in baffles tubes, *Chem. Sci. Eng.*, Vol. 50, No. 14 (1995) (2211-2224)

Ueda, Y.; Biwa, T.; Mizutani, U. & Yazaki, T. (2004). Experimental studies of a thermoacoustic Stirling prime mover and its application to a cooler, *J. Acoust. Soc. Am.* , Vol. 115, No. 3, (March 2004), (1134-1141)

Velazquez, A.; Arias, J.R. & Mendez, B. (2007). Laminar heat transfer enhancement downstream of a backward facing step by using a pulsating flow, *Heat Mass Transfer* (2007)

Wakeland, R. S. & Keolian, R.M. (2004a). Calculated effects of pressure-driven temperature oscillations on heat exchangers in thermoacoustic devices with and without a stack, *J. Acoust Soc. Am.* , Vol. 116, No. 1, (July 2004), (294-302)

Wakeland, R.S. & Keolian, R.M. (2004b). Efectiveness of parallel-plate heat exchangers in thermoacoustic devices, *J. Acoust. Am.*, Vol. 115, No. 6, (June 2004), (2873-2886)

Xiongwei N. & Pereira N. E. (2000). Parameters affecting fluid dispersion in a continuous oscillatory baffled tube, *AIChE Journal*, Vol. 46, No. 1 (2000) (37-45)

Yu, J.C.; Li, Z.X. & Zhao, T.S. (2004). An analytical study of pulsating laminar heat convection in a circular tube with constant heat flux, *Int. J. Heat Mass Transfer*, Vol. 47 (2004) (5297-5301)
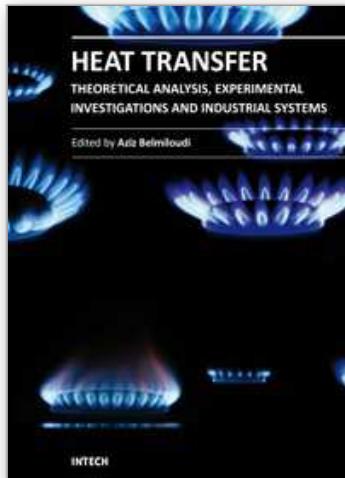
Heat Transfer - Theoretical Analysis, Experimental Investigations and Industrial Systems

Edited by Prof. Aziz Belmiloudi

Over the past few decades there has been a prolific increase in research and development in area of heat transfer, heat exchangers and their associated technologies. This book is a collection of current research in the above mentioned areas and discusses experimental, theoretical and calculation approaches and industrial utilizations with modern ideas and methods to study heat transfer for single and multiphase systems. The topics considered include various basic concepts of heat transfer, the fundamental modes of heat transfer (namely conduction, convection and radiation), thermophysical properties, condensation, boiling, freezing, innovative experiments, measurement analysis, theoretical models and simulations, with many real-world problems and important modern applications. The book is divided in four sections : "Heat Transfer in Micro Systems", "Boiling, Freezing and Condensation Heat Transfer", "Heat Transfer and its Assessment", "Heat Transfer Calculations", and each section discusses a wide variety of techniques, methods and applications in accordance with the subjects. The combination of theoretical and experimental investigations with many important practical applications of current interest will make this book of interest to researchers, scientists, engineers and graduate students, who make use of experimental and theoretical investigations, assessment and enhancement techniques in this multidisciplinary field as well as to researchers in mathematical modelling, computer simulations and information sciences, who make use of experimental and theoretical investigations as a means of critical assessment of models and results derived from advanced numerical simulations and improvement of the developed models and numerical methods.

How to reference

In order to correctly reference this scholarly work, feel free to copy and paste the following:

INTECH
open science | open minds

51000 Rijeka, Croatia
Phone: +385 (51) 770 447
Fax: +385 (51) 686 166
www.intechopen.com

中国上海市延安西路65号上海国际贵都大饭店办公楼405单元
Phone: +86-21-62489820
Fax: +86-21-62489821